

# Circular Foreign Object Detection in Chest X-ray Images

Fatema Tuz Zohora and K.C. Santosh

Dept. of Computer Science, The University of South Dakota  
414 E Clark St, Vermillion, SD 57069

`fatema.zohora@coyotes.usd.edu` and `santosh.kc@usd.edu`

**Abstract.** In automated chest X-ray screening (to detect i.e, Tuberculosis for instance), the presence of foreign objects (buttons, medical devices) hinders it's performance. In this paper, we present a new technique for detecting circular foreign objects, in particular buttons, within chest X-ray (CXR) images. In our technique, we use a pre-processing step that enhances the CXRs. Using these enhance images, we find the edge images performing four different edge detection algorithms (Sobel, Canny, Prewitt, and Roberts) and after that, we apply some morphological operations to select candidates (image segmentation) in the chest region. Finally, we apply circular Hough transform (CHT) to detect the circular foreign objects on those images. In all tests, our algorithm performed well under a variety of CXRs. We also compared our proposed technique's performance with existing techniques in literature (Viola-Jones and CHT). Our technique was able to excel performance in terms of both detection accuracy and computation time.

**Keywords:** chest x-ray (CXR) images, foreign object detection, edge detection, button detection, circular Hough transform (CHT), Viola-Jones.

## 1 Introduction

### 1.1 Context

Lung diseases are major threats because significant numbers of people suffer from these diseases such as tuberculosis [12], pneumonia, lung cancer and pulmonary edema across the world. The advent of new powerful hardware and software techniques has triggered attempts to develop computer-aided diagnostic (CAD) systems for automatic chest x-ray screening [11] [13] [14]. However, foreign objects such as buttons on the gown that the patients were wearing or coins/buttons mistakenly swallowed by patients, within the chest x-ray images hinders the performance of the automatic screening process. Fig. 1 shows one such CXR which contain several buttons and Fig. 2 shows a closer view of all the buttons in these CXRs. The presence of such objects (especially the ones located within the lung region) hinder the CAD system performance, as they are not due

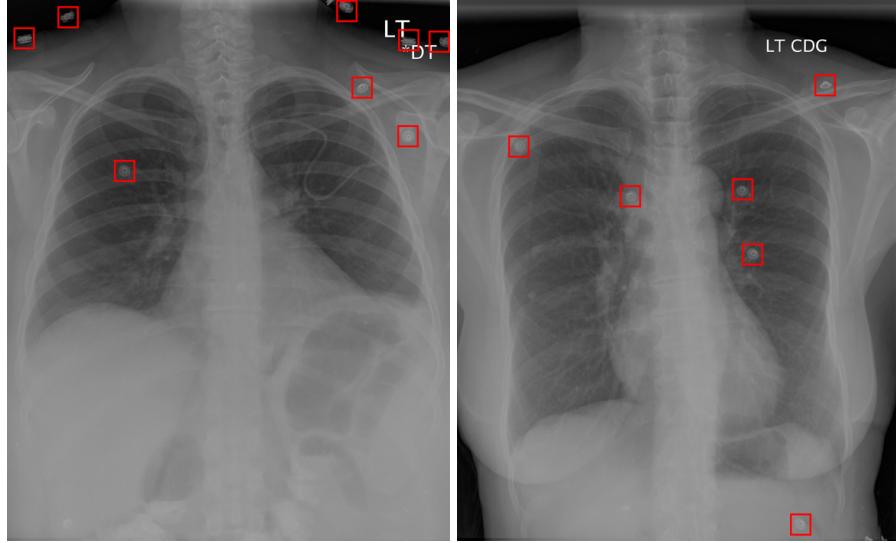


**Fig. 1.** CXRs containing buttons, boxes marked by red indicate the location of buttons in the images.

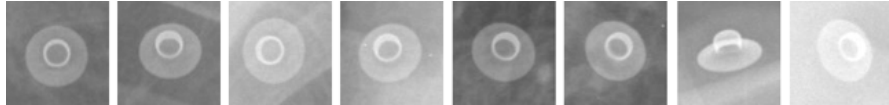


**Fig. 2.** Closer view of all the buttons in above chest x-ray images.

to any lung abnormalities and therefore should not be considered. Therefore, in the screening process precise detection of foreign objects is an important issue for screening of chest diseases in CAD systems.

## 1.2 Related works and our contributions

Detecting foreign objects in CXRs is a challenging and open research problem. It does not have rich state-of-the-art. In [1], Xue et al. used techniques Viola-Jones and circular Hough transform (CHT) for circular object detection in CXRs. Among them, CHT algorithm has average recall and precision rate and its performance depends on the image intensity. If there is not enough contrast between the objects (buttons in CXRs) and the background image, then the performance of CHT degrades drastically. On the other hand, Viola-Jones algorithm has high false detection rate, which is confusing for the CAD system.

To improve the CAD systems, precise and faster methods require. Unlike [1], we enhance the circular candidate objects from the CXRs applying edge detection, followed by some morphological operations, and then perform CHT on these enhanced circular candidates (see Section 2). We compared the perfor-

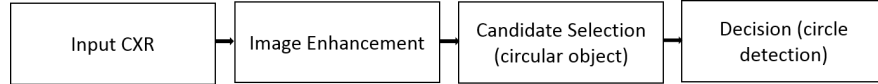


**Fig. 3.** Workflow: It begins with image enhancement, using intensity normalization and image adjustment. After that candidate (circular object) selection is performed and finally decision is made whether the candidates are circular shape objects.

mance for four different edge detection algorithms. Finally, we compared our proposed method with the two benchmarking techniques that are used in [1]. In all our tests, the proposed algorithms showed better performance the other existing techniques and achieved 100% precision and 100% recall <sup>1</sup>.

### 1.3 Organization of the paper

The rest of this paper is structured as follows: In Section 2, we give detailed overview of our proposed technique. At first, we briefly discuss the image enhancement (see Section 2.1) and then we provide a detailed description of the circular object detection process (see Section 2.2). Next, Section 3 provides information about the data set and the evaluation protocol (see Section 3.1) and results (see Section 3.2). Finally, Section 4 concludes the paper.

## 2 The proposed technique

In our algorithm, we first enhance the CXRs to increase the contrast between the button objects with their background, using intensity normalization and image adjustment. Next, we apply candidate selection (CS)/circular shape enhancement step to make the circular candidates more distinct and then we perform Circular Hough Transform (CHT) for extracting circular shape objects (e.g., buttons) in these images. For improving the performance, we segment the chest area to identify the region of interest. Fig. 3 briefly presents the proposed method workflow.

### 2.1 Image enhancement

We applied some pre-processing steps on the CXRs to improve the image quality, so that the objects of interest (e.g., buttons) become more evident. The quality of the pre-processing steps strongly affects the performance of the subsequent circular object detection steps.

In our tests, we applied two pre-processing steps: intensity normalization and image adjustment. For intensity normalization, we used the same approach as in [1]. For image adjustment; however, we adopted slightly different approach

---

<sup>1</sup> Note that, we have tested using 50 CXR images.

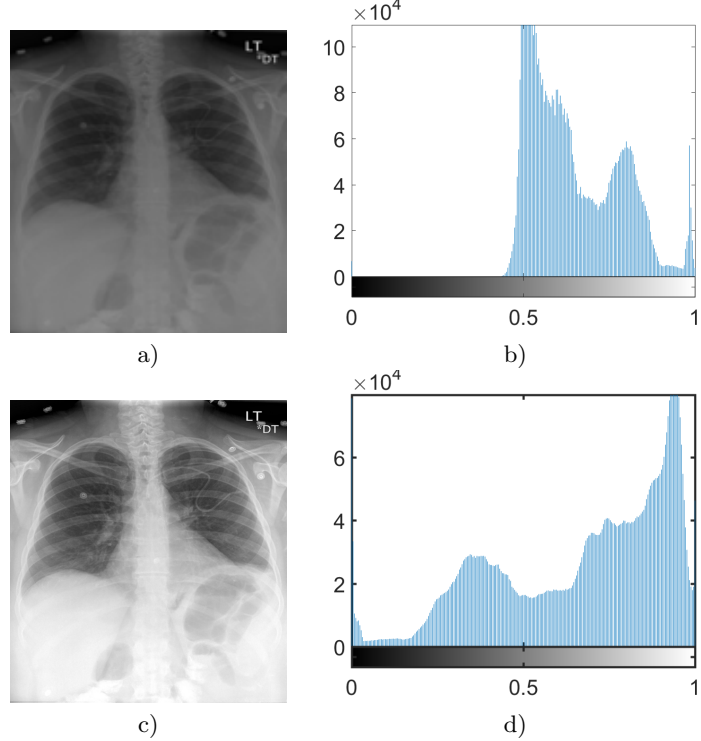


**Fig. 4.** Image Enhancement: a) original image, b) original image histogram, c) enhanced image, and d) enhanced image histogram.

than [1]. For images without any windowing (intensity window manually optimized by radiologists to visually enhance the lung tissue region) information, [1] performs adjustment only for low contrast images. We, however, observed that applying such adjustments always improve performance. Hence, we applied it as a common pre-processing step to all images.

Fig. 4 shows one such low contrast input and the resultant image after enhancement. It also shows the histogram of pixel intensities before and after the adjustment. It can be seen from the figure that the adjusted image has more uniformly distributed intensity values and a higher contrast.

## 2.2 Candidate (circular object) selection

By analyzing the input CXRs, we observe that the buttons in the lung region are mostly of circular/elliptical shape and their boundaries are sharper than other areas. Based on these facts, we extracted circular shape object from CXRs. In our proposed technique, we applied edge detection and then performed some morphological operations on these edge-images to enhance the circular candidates for candidate selection.

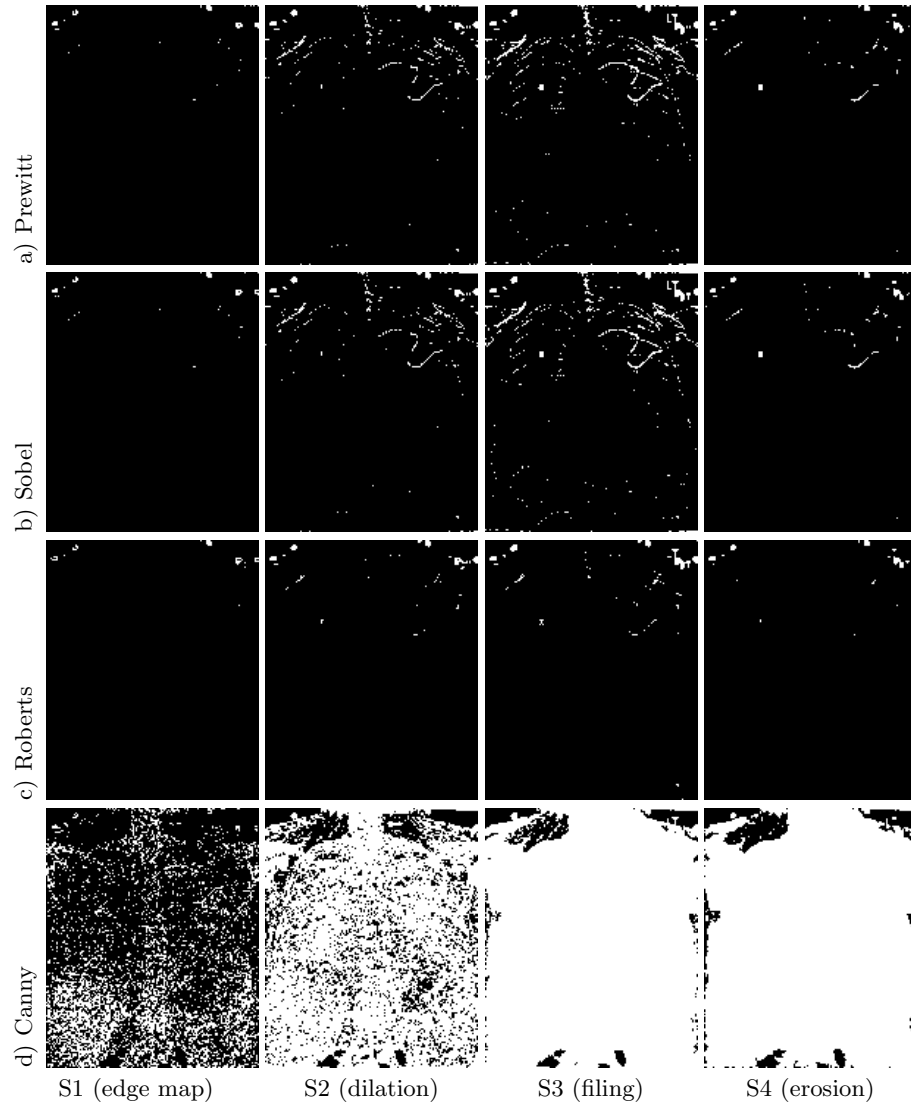


**Fig. 5.** Candidate selection: a), b), c), and d) show results for Prewitt, Sobel, Roberts, and Canny edge detection correspondingly. Steps S1, S2, S3, and S4 correspond to the edge detection, dilation, filling, and erosion.

**Edge detection.** We applied edge detection to extract high gradient regions in the image. For this, we tested with four edge detection operators: Canny [5], Prewitt [6], Sobel [7], and Roberts [8]. Fig. 5 S1 represents the four resultant edge-images.

Now, we apply several morphological operations [9] on the edge-images to segment and enhance all distinct objects in the image.

**Dilation.** We first threshold the edge images to create binary edge masks. Such binary edge masks usually mark the object boundaries in the image. However, due to noise or low background to foreground contrast, the edge mask in general is not continuous and hence the corresponding object boundaries have small gaps in between. To overcome this issue, we dilated the edge mask using line shaped structuring elements. We used two linear structuring element **Sl1** and **Sl2** of length 3, oriented at angles 90° and 0° correspondingly.

$$\mathbf{Sl1} = \begin{bmatrix} 1 \\ 1 \\ 1 \end{bmatrix} \quad , \quad \mathbf{Sl2} = [1 \ 1 \ 1] \quad \text{and} \quad \mathbf{Sd} = \begin{bmatrix} 0 & 1 & 0 \\ 1 & 1 & 1 \\ 0 & 1 & 0 \end{bmatrix}$$

**Filling.** In this step, we first label all the connected objects in the dilated image. Next, for each such object we perform a flood-fill operation that fills the holes in the objects and generates objects with solid interior.

**Erosion.** In order to remove noisy small object from the edge images, next we eroded the image. For erosion, we used a diamond-shaped structuring element **Sd**. In this step, we also suppress structures that are connected to the image border. After these steps, we apply CHT for button extraction. Fig. 5 S1-S4 shows the step-wise outputs of the circular object enhancement process.

### 2.3 Decision (circle detection)

In our experiments, we used the size invariant circle detection method [2] for detecting circle on candidate selection image.

Our goal is to detect circular shape objects in the lung region of the CXRs, since that is the main area of interest for detecting chest diseases in the CAD systems. The accuracy of the lung segmentation has a big impact on the overall performance of the system. For lung segmentation, we applied anatomical atlases with nonrigid registration algorithm [4]. In Fig. 6, shows the intermediate resultant circular objects detection on candidate selection image with and without lung segmentation. In Fig. 7 a), shows the complete view of circular foreign object detection on candidate selection image with lung segmentation.

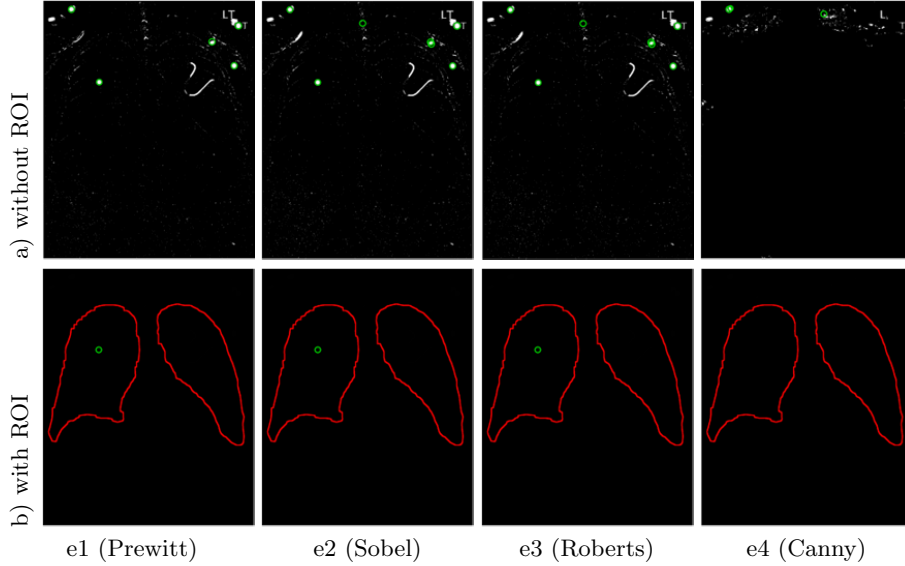


**Fig. 6.** Decision: e1, e2, e3, and e4 correspond to the Prewitt, Sobel, Roberts and Canny edge images followed by circular object selection steps with CHT. a) and b) show resultant circular object detection intermediate step without and with region of interest (ROI) respectively. Circles marked by green indicate the location of circular shape object on the candidate selection images.

### 3 Experiments

#### 3.1 Dataset, evaluation protocol, and metrics

In our study, we used subset of data-set maintained by National Library of Medicine which is composed of 50 DICOM images. This subset of data set has total 32 buttons in chest area. We annotated corresponding ground-truths, since they are not available in this data set.

We used precision and recall to measure the performance.

$$Precision = \frac{TP}{TP + FP} \quad and \quad Recall = \frac{TP}{TP + FN}$$

where TP = true positive (accurately detected buttons in the chest area), FP = false positive (inaccurately detected buttons), and FN = false negative (undetected buttons). The following section presents a summary of the experimental setup, test and quick comparison.

#### 3.2 Results and analysis

In our proposed technique, we applied four different edge operations and additional circular object enhancement step is performed on these edge images.

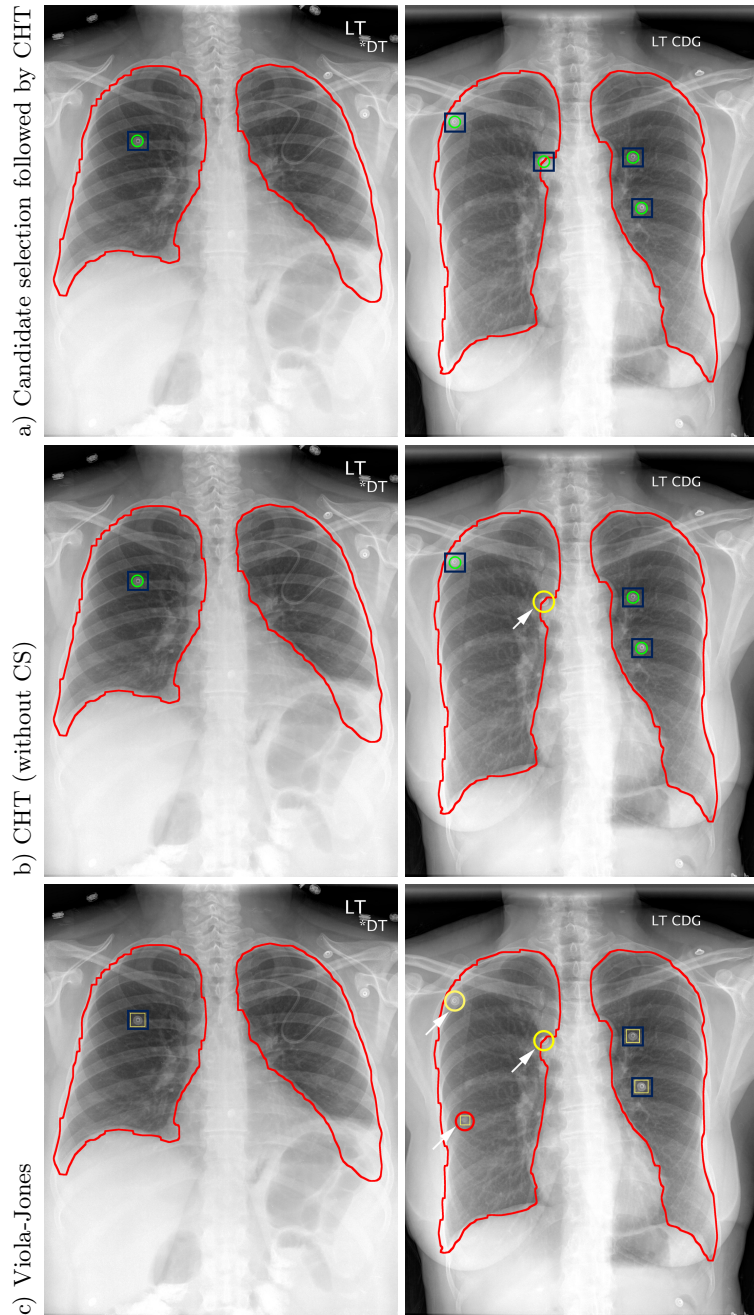


**Fig. 7.** Circular object detection: a), b) and c) show candidate (circular object) selection (CS) followed by CHT, CHT and Viola-Jones respectively. Here, circles marked by yellow pointed by white arrow indicate false negative, circles marked by red pointed by white arrow indicate false positive and rectangles marked by blue indicate true positive.

**Table 1.** Circular foreign object detection result: Candidate selection (CS) followed by CHT

Ground-truth	Detection	TP	FP	FN	Precision	Recall
32	32	32	0	0	1.0	1.0

**Table 2.** Circular foreign object detection result: CHT (without CS)

Ground-truth	Detection	TP	FP	FN	Precision	Recall
32	22	22	0	10	1	0.69

**Table 3.** Circular foreign object detection result:: Viola-Jones

Test	Train	Ground-truth	Detection	TP	FP	FN	Precision	Recall
10	40	7	9	6	3	1	0.67	0.86
20	30	18	17	12	5	6	0.71	0.67
30	20	22	22	17	5	5	0.77	0.77
40	10	27	13	11	2	16	0.85	0.41

**Table 4.** Computational time of button detection techniques

Method	Time(in sec)
CS followed by CHT	8.52
Viola-Jones	18.83
CHT	29.02

Fig. 5 S1-S4 shows all four steps of this approach. It can be seen from the S4 step of the figure that Prewitt edge detection performs the best with distinct circular objects and less amount of outlier high gradient regions. It also is the fastest method, due to the less amount of high gradient regions. Sobel operator also had similar strong circular objects but it had more outlier high gradient regions too, which leads to false detection and more computation time. On the other hand, Roberts does not have distinct circular objects. However, Canny performs the worst with this approach, because Canny edge-image has many strong connected object all over the image. Hence, after the dilation and filling steps a big portion of the image gets filled and CHT does not work well on such images. Hence, we only include results of this approach with Prewitt edge-images. The computation time is presented in Table 4 and the detection performance in Table 1. Fig. 7 a) shows circular foreign object detection results for this approach. Applying this method, we got 100% precision and 100% recall using Prewitt edge image.

Now, we compare our result with two benchmarking techniques Viola-Jones and CHT that are used in [1] for circular object detection.

For CHT algorithm, we followed similar approach as in [1] and used the implementation in MATLAB image processing toolbox. However, instead of using

a single radii range, we used a set of three radii ranges ([12, 19], [25, 45] and [46, 60]) and accumulated the results. It not only increases the speed but also accuracy of the detection process. Figure 7 b) shows two output images of this algorithm and Table 2 presents a summary of the results.

For Viola-Jones [3] algorithm, we also applied similar approach in [1]. Due to data set of 50 DICOM CXRs, we trained it using 50 positive images and 50 negative images, and set the number of cascade stages to 6. We observed that Viola-Jones detector perform best using Haar-like feature. Table 3 provides a comparison of the results for this method while varying the number of training and testing images. Figure 7 c) shows two of the resultant outputs of this method.

We also measured the computational time for all circular object detection techniques. Our system has following configuration: intel core i7 processor, windows 7 operating system and MATLAB R2016a. We calculated computational time in seconds per image, on average. Average CXR size is around 3K x 3K. Table 4 shows the computational time of all circular object detection techniques. Note that in [1], authors did not report computational time.

## 4 Conclusion

In this work, we have focused on identifying circular foreign objects such as buttons appearing in lung regions of the chest X-ray images. We presented a novel technique for circular foreign object detection. Our proposed technique is encouraging, both in terms of detection accuracy and computation time. Using Prewitt edge detection followed by circular candidate selection and CHT, we achieved perfect detection of 100% precision and recall. As future work, we plan to test the robustness of our algorithms on larger data sets and extend this work to detect other types of circular and non-circular foreign objects (e.g., medical tubes) that usually appears in CXRs.

## References

1. Xue, Z., Candemir, S., Antani, S., Long, L. R., Jaeger., S., Demner-Fushman, D., Thoma, G. R.: Foreign object detection in chest X-rays. Bioinformatics and Biomedicine (BIBM), 2015 IEEE International Conference on. pp. 956–961, IEEE, (2015)
2. Atherton, Tim J and Kerbyson, Darren J: Size invariant circle detection, Image and Vision computing, vol. 17, num. 11, pp. 795–803, Elsevier, (1999)
3. Viola, P., Jones, M.: Rapid object detection using a boosted cascade of simple features. Computer Vision and Pattern Recognition, 2001. CVPR 2001. Proceedings of the 2001 IEEE Computer Society Conference on, vol. 1, pp. I–511, IEEE, (2001)
4. Candemir, S., Jaeger, S., Palaniappan K., Musco, J. P., Singh, R. K., Xue, Z., Karargyris, A., Antani, S., Thoma, G., McDonald, C. J.: Lung segmentation in chest radiographs using anatomical atlases with nonrigid registration, Medical Imaging, IEEE Transactions on, vol. 33, num. 2, pp. 577–590, IEEE, (2014)

5. Canny, J.: A computational approach to edge detection. *Pattern Analysis and Machine Intelligence, IEEE Transactions on*, num. 6, pp. 679–698, IEEE, (1986)
6. Prewitt, J. M.: Object enhancement and extraction, *Picture processing and Psychopictorics*, vol.10, num. 1, pp. 15–19, Academic Press, New York, (1970)
7. Sobel, I.: History and definition of the sobel operator, Retrieved from the World Wide Web, (2014)
8. Lawrence, G. R.: Machine perception of three-dimensional solids, Ph. D. Thesis, Massachusetts Institute of Technology Cambridge, MA, USA, (1963)
9. Soille, P.: Morphological image analysis: principles and application, Springer Science & Business Media, (2013)
10. Davies, E. R.: Machine vision: theory, algorithms, practicalities. Chapter 10. 3rd Edition. Elsevier, (2004)
11. Schaefer-Prokop, C., Neitzel, U., Venema, H. W., Uffmann, M., P., Mathias: Digital chest radiography: an update on modern technology, dose containment and control of image quality, *European radiology*, vol.18, num. 9, pp. 1818–1830, Springer, (2008)
12. World Health Organization (WHO).: global tuberculosis report (2014)
13. Santosh, K. C., Vajda, Szilárd., Antani, Sameer., Thoma, George R.: Edge map analysis in chest X-rays for automatic pulmonary abnormality screening, *International Journal of Computer Assisted Radiology and Surgery*, pp. 1–10, issn. 1861-6429, (2016)
14. Karargyris, A., Siegelman, J., Tzortzis, D., Jaeger, S., Candemir, S., Xue, Z., Santosh, KC., Vajda, Szilárd., Antani, Sameer., Folio, L., others: Combination of texture and shape features to detect pulmonary abnormalities in digital chest X-rays, *International journal of computer assisted radiology and surgery*, vol.11, num.1, pp. 99–106, Springer (2016)